

Modeling of relaxation oscillations in CO oxidation on metallic catalysts with consideration of reconstructive heterogeneity of the surface

E.A. Ivanova^a, N.A. Chumakova^{a,*}, G.A. Chumakov^b, A.I. Boronin^a

^a Borekov Institute of Catalysis SB RAS, Pr. Akad. Lavrentieva 5, 630090 Novosibirsk, Russia

^b Sobolev Institute of Mathematics SB RAS, pr. Akad. Koptyuga 4, 630090 Novosibirsk, Russia

Abstract

This paper is devoted to the development of a low-dimensional kinetic model of CO oxidation on a metallic catalyst surface and theoretical study of arising nonlinear phenomena and relaxation oscillations of the reaction rate. Experimental results of studies on the adsorbed oxygen are presented and its significance in the CO oxidation mechanism on Ir catalyst is shown. We consider the conventional Langmuir–Hinshelwood mechanism of catalytic CO oxidation and take into account the possibility of a metallic surface modification during reaction due to the oxygen penetration into subsurface layers. We suggest that when the adsorbed oxygen concentration exceeds some critical value, a surface modification occurs and the reaction capability of adsorbed oxygen changes, so that the activation energy of the interaction between the adsorbed species sharply increases. Construction of bifurcation curves on the parametric plane (P_{CO} , P_{O_2}) permits us to separate areas of CO and O₂ partial pressures, for which self-oscillations and/or multiplicity of steady states appear. This paper deals with parametric analysis of a new two-variable kinetic model of CO oxidation on Ir catalyst surface, but the approach developed is rather general and can be applied to studies of different catalytic reactions.

© 2004 Elsevier B.V. All rights reserved.

Keywords: Catalytic reaction; Oscillations; Kinetic model; Surface modification; CO oxidation

1. Introduction

CO oxidation on the surface of metals of the platinum group is a model reaction in which the main fundamental aspects of heterogeneous catalysis are verified. Nowadays, a popular trend is construction of a heterogeneous catalytic reaction mechanism on the atomic-molecular level by taking into account the dynamic nature of the surface. Due to inherent dynamic variations of the catalyst surface under the reaction conditions, the critical phenomena such as steady state multiplicity, oscillations and chaotic behavior of catalytic reaction rate are observed [1–8,15–16].

The existence of such critical phenomena in heterogeneous catalytic reactions helps us to determine a more reliable reaction mechanism and gives better understanding of the physical–chemical processes in the “reaction medium–catalyst” system. The most important factor in cat-

alytic CO oxidation is the interaction of oxygen with metallic surface. Due to the reconstructive properties of the open and stepped planes on the platinum metals, some oxygen atoms can reconstruct the surface and/or penetrate into the subsurface layers, and cause both structural and chemical modification of the adsorption sites. These processes are in charge of the discrete change in the rate constants of elementary reactions. In this paper, we present some interesting experimental results obtained by means of the thermo programmed reaction (TPR) and X-ray photoelectron spectroscopy (XPS) techniques applied to study the adsorbed oxygen and its role in the reaction mechanism of deep oxidation. The photoelectron spectroscopy is the most reliable tool for exact identification of surface oxygen species [7,8]. Together with other methods that give information on reactivity of the adsorbed species (thermal desorption (TDS), TPR, and others), the XPS gives the experimental data to create a rather detailed reaction mechanism.

Earlier, the experimental study of the oxygen states on Ir surface and their interaction with CO was carried out

* Corresponding author. Tel.: +7 383 230 62 78; fax: +7 383 230 68 78.
E-mail address: chum@catalysis.nsk.su (N.A. Chumakova).

under conditions of ultrahigh vacuum [9]. Kinetic scheme and model of CO oxidation that was suggested consists of 12 elementary reactions and five differential equations, respectively [10,11]. This model was found to be rather effective, able to describe some experimental data and to predict multiplicity of steady states, existence of critical phenomena and harmonic self-oscillations of the reaction rate near the Hopf bifurcation points. However, because of the high dimension of the ordinary differential equations system, the model appeared too complex. The qualitative analysis of the reaction dynamics by means of methods of the dynamical systems theory has not been carried out.

To solve such kind of problems we suggest a hierarchical approach to theoretical study of the dynamics of nonlinear kinetic models. The method is based on the distinction of slow and fast variables (or some combinations of variables) in the model. It has been successfully applied to the study of the hydrogen and oxygen interaction over metallic catalysts [12,13]. We described complex dynamic behavior of the three-variable heterogeneous kinetic system using the results obtained for several models with lower number of variables (sub-models of low dimension).

This paper is devoted to the development of a new low-dimensional kinetic model for heterogeneous CO oxidation on the Ir catalyst surface and theoretical investigation of arising nonlinear phenomena using hierarchical approach. Now we propose a two-variable model, which allows us to find relaxation oscillations of the reaction rate and give the parametric analysis of the oscillations.

2. Experimental part

The experiments were carried out with the photoelectron spectrometer “VG ESCALAB HP” produced by VG Scientific (Great Britain). The spectrometer equipped with X-ray source with the double Mg/Al anode that permits us to use for excitation the primary radiation of Mg $K\alpha$ and Al $K\alpha$ ($h\nu = 1253.6$ and 1486.6 eV, respectively). At the start and after finish of each set of the experiments the spectrometer calibration was done relative to the standard lines Au $4f_{7/2}$ ($E_b = 84.0$ eV) and Cu $2p_{3/2}$ ($E_b = 932.7$ eV) [14]. The value of Ir $4f_{7/2}$ bond energy of 60.7 eV was used as an inner standard [8].

For simultaneous application of the experimental methods, namely X-ray photoelectron spectroscopy (XPS), thermal desorption (TDS) and thermo programmed reaction (TPR), the quadrupole mass-spectrometer was installed in the analyzer chamber. Measuring of CO + O₂ steady state reaction rate on Ir has been performed with calibration of mass-peaks on pressure measured with Byard-Alpert gauge.

The polycrystalline iridium foil was used, surface of which was cleaned with cycles of ion bombardment, oxygen adsorption and high-temperature annealing. The surface cleanliness was controlled with XPS method.

3. Experimental results

The stationary reaction kinetic data in dependence on the temperature at different ratios of the O₂ and CO pressures are presented in Fig. 1. We show both the reaction rate and adsorbed CO and oxygen concentrations calculated from the XPS spectra obtained simultaneously with the mass-spectra. Obviously, if the reaction proceeds under CO excess (Fig. 1a and d) the temperature dependencies of the reaction rate and adsorbates concentrations are rather smooth in a wide temperature interval. Oxygen is practically not accumulated on the surface even at very high temperature $T > 700$ K. Under increasing the oxygen pressure in the reaction mixture (Fig. 1b and e) the behavior of the reaction rate and the adsorbates concentrations changes so that the corresponding curves become more sharp, the reaction rate increase occurs at low temperatures, and the surface coverage with adsorbed oxygen achieves 25% of the monolayer. The substantial observation is that during cooling of the sample the reversible reaction behavior occurs without a hysteresis. Hysteresis of both the reaction rate and concentration occur in the case when the P_{O_2}/P_{CO} ratio is equal to 9 (Fig. 1c and f), and adsorbed oxygen is accumulated up to the very high surface coverage of about 2/3 monolayer.

These kinetic data obtained in the regime in situ under steady state conditions illustrate well enough the fact that the adsorbed oxygen plays a key role for forming the hysteresis phenomena in CO oxidation reaction due to the influence of the oxygen atoms on the iridium surface properties. Ertl [15] and King [16] studied the CO oxidation mechanism on Pt (100) surface and made a conclusion concerning the leading role of adsorbed CO in passing of the self-oscillation processes. However, the Pt (100) plane is rather an exception to the rule. We suggest that leading role in generation and keeping of self-oscillations belongs to the atomic oxygen because, at first, of the larger bonding strength with metal and, secondly, due to the possibility of subsurface oxygen forming and carrying the reconstructive influence on the metal surface layer [8,15–19].

For confirmation of the above-stated propositions, in Fig. 2 we present some results of oxygen adsorption studies on the polycrystalline iridium surface obtained by means of a combination of XPS and TPR methods. One can compare the oxygen properties after O₂ adsorption with equal exposure ($\varepsilon(O_2) = 3$ L) at 300 and 800 K. It can be seen, that O₂ adsorption at 800 K leads to an essentially lesser integral intensity of O 1s line (Fig. 2a, curve 2) in comparison with O₂ adsorption at 300 K (Fig. 2a, curve 1). The thermo programmed reaction O_{ads} + CO_{ads} in adsorption layer in which oxygen has been adsorbed at 300 K, leads mainly to one peak at 400 K and weakly expressed shoulder at 500–600 K (Fig. 2b, curve 1). In the case of preliminary O₂ adsorption at 800 K, the CO₂ forming due to O_{ads} + CO_{ads} is characterized by two discrete maximum at 400 and 600 K (Fig. 2b, curve 2). In both cases a flash of adsorption layer led to removal of practically all

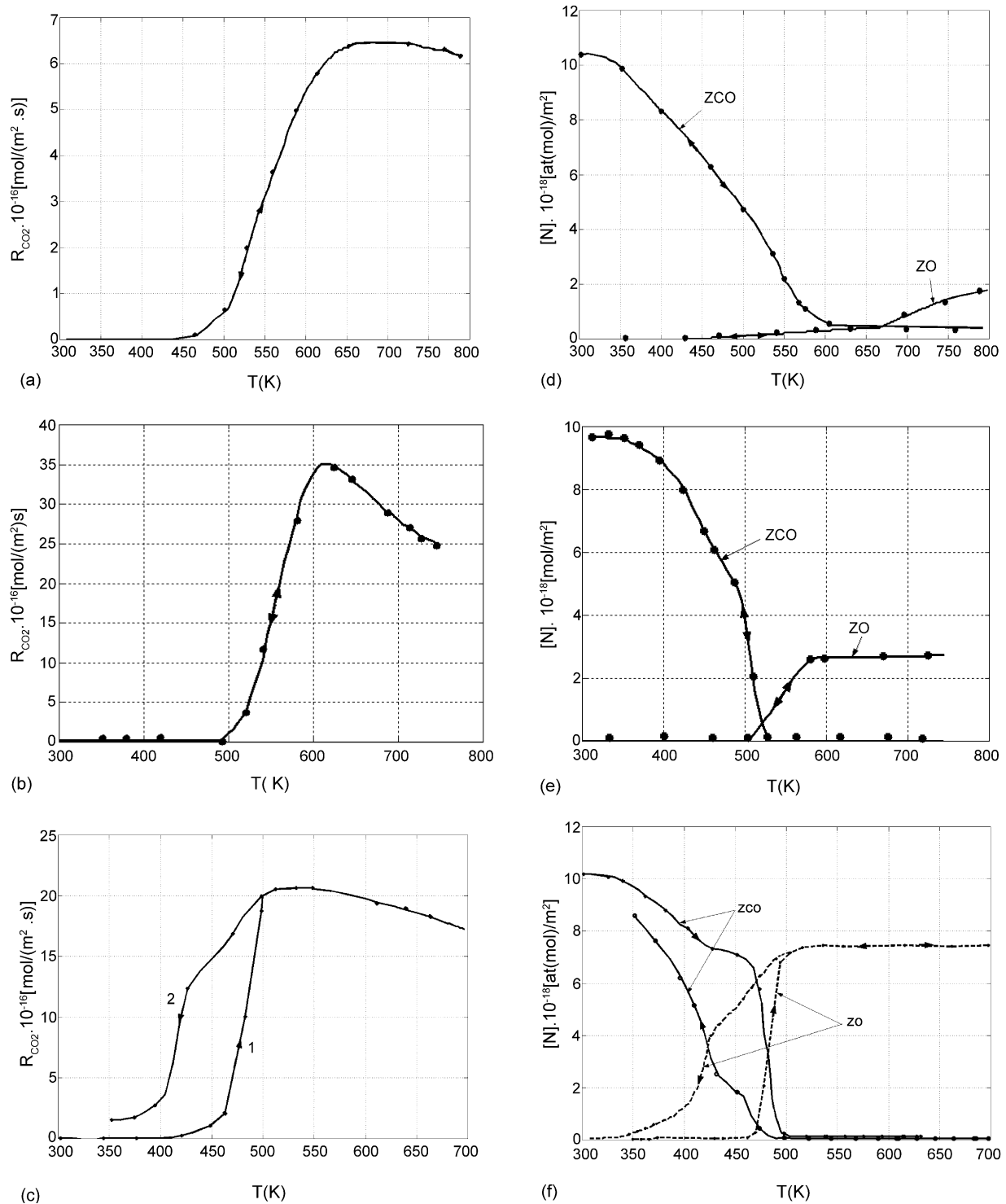


Fig. 1. Dependencies of reaction rate (a–c) and surface concentrations of CO and oxygen (d–f) on temperature at $P_{O_2}/P_{CO} = 1/3$ (a and d); $P_{O_2}/P_{CO} = 2$ (b and e) and $P_{O_2}/P_{CO} = 9$ (c and f) under heating (arrows to the right) or cooling of the sample (arrows to the left).

pre-adsorbed oxygen if the amount of adsorbed carbon oxide was more than the oxygen amount. Fig. 2b shows that this penetration process leads to a very significant decreasing of the oxygen reactivity and therefore to appearance in TPR spectra the high-temperature peak at 600 K. The penetration of oxygen atoms into the metallic surface layer finished at

about 700 K, and the transition rate is so high, that it is comparable with oxygen and CO interaction rate in the adsorbed layer.

Thus, the adsorbed oxygen on iridium is nonuniform. A detailed 12-stages kinetic scheme was suggested earlier in [9–11] which includes all types of interactions between ad-

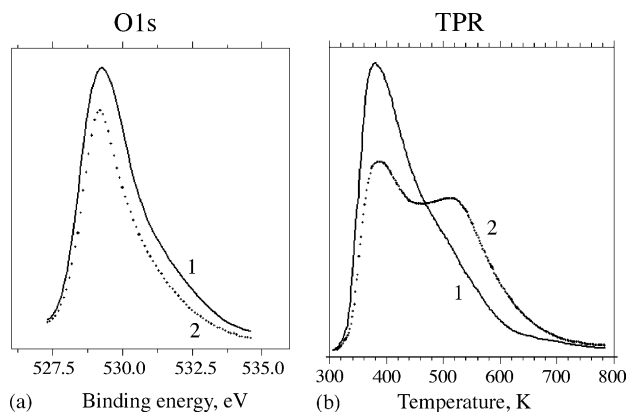
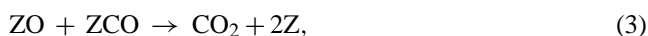


Fig. 2. Oxygen adsorption on the polycrystalline iridium surface studied by combination of XPS and TPR methods: (a) O 1s spectra after O₂ adsorption with equal exposure $\varepsilon(\text{O}_2) = 3 \text{ L}$, (b) TPR spectra of CO₂ evolution after O₂ pre-adsorption with $\varepsilon(\text{O}_2) = 3 \text{ L}$ and following CO adsorption up to the surface saturation. Curves 1 correspond to the temperature 300 K while curves 2 were obtained at 800 K.

sorbed CO and oxygen and the phenomenon of oxygen penetration into the subsurface layer as well. However, as it is pointed above, such detailed scheme increases greatly the dimension of the kinetic model and restricts the qualitative mathematical study. In order to account for effects of oxygen penetration and discrete change of the surface properties and to keep a low dimension of the mathematical model, now we propose a new methodological approach. It consists in a step-wise change of parameters of the reagents interaction stages depending on the surface oxygen concentration. The basis for such approach is a large amount of the literature data concerning the reconstructive properties of metal surfaces and formation of the “subsurface” type oxygen. These two phenomena, first of all, are responsible for changing the reagents interaction due to a discrete changing of the reagents states on the surface. Assuming that the acts of the metal surface reconstruction or the oxygen penetration into the metallic subsurface layer are extended on a limited space, we can assume with a good accuracy the process of such structure transition be very localized, and states of oxygen and CO be energy-wise discrete. Nowadays, the approach of “discrete states” in processes of surface reconstruction and reactions over a metal surface becomes more and more prevalent and usable in the surface chemistry for dynamic processes description [8,15–19].

4. Kinetic scheme and mathematical model – I

Let us consider the classical Langmuir–Hinshelwood mechanism of CO oxidation on the metallic catalyst surface:



where ZO and ZCO are the intermediate compounds of oxygen and CO on the Ir surface, Z is an active site on the catalyst surface, CO, O₂ and CO₂ are the species in the gas phase.

Starting with the system (1)–(3), we can write a kinetic model that describes dynamic behavior of dimensionless concentrations of CO (x) and oxygen (y) adsorbed on the catalyst surface assuming that properties of the surface do not depend on x and y :

$$\begin{aligned} x' &= k_1(1 - x - y) - k_{-1}x - k_3xy \equiv P(x, y), \\ y' &= 2k_2(1 - x - y)^2 - k_3xy \equiv Q(x, y). \end{aligned} \quad (4)$$

The reaction constants depend on both temperature T and partial pressures P_{CO} and P_{O_2} as follows [10]:

$$k_1 = k_{10}P_{\text{CO}}, \quad k_2 = k_{20}P_{\text{O}_2},$$

$$k_{-1} = k_{-10} \exp\left(-\frac{E_1}{RT}\right),$$

$$k_3 = k_{30} \exp\left(-\frac{E_3}{RT}\right).$$

Consider the region $\Omega = \{(x, y): x \geq 0, y \geq 0, x + y \leq 1\}$. Note that if the initial point (x_0, y_0) at $t = 0$ is in Ω then $(x, y) \in \Omega$ for all $t > 0$, i.e. Ω is a trapping region in the (x, y) -plane. The study of the model was carried out for the following parameters [9,10]:

$$k_{10} = 3.6 \times 10^5 \text{ s}^{-1} \text{ Torr}^{-1}, \quad k_{-10} = 10^{13} \text{ s}^{-1},$$

$$k_{20} = 0.9 \times 10^5 \text{ s}^{-1} \text{ Torr}^{-1}, \quad k_{30} = 10^{13} \text{ s}^{-1},$$

$$E_1 = 35 \text{ kcal mol}^{-1}.$$

The range of the activation energy E_3 is 28–33 kcal mol⁻¹ and the temperature T is 400–500 K. We study the model for P_{CO} and P_{O_2} in the range of 10⁻⁸ to 10⁻⁶ Torr.

It is known that the model (4) permits qualitative interpretation of the steady states multiplicity. There are no more than three steady states exist with $x, y > 0$ and $x + y < 1$. Note that the unstable steady state $x_s = 0, y_s = 1$ (a saddle point) exists in the model (4) for all parameters values and the stable manifold of this point lies outside the region Ω . In what follows we will only consider the steady states of the system (4) that lie inside the region Ω .

The steady states dependence on the temperature is shown in Fig. 3. At $E_3 = 33 \text{ kcal mol}^{-1}$ there is a unique steady state for all temperatures considered. At the lower activation energy $E_3 = 28 \text{ kcal mol}^{-1}$, the steady state multiplicity takes place for some intermediate temperatures, i.e. it is possible to find two stable steady states (sinks) and an unstable one (a saddle) inside Ω .

These steady states were found numerically using Newton’s method. The stability of each steady state was determined by computing the eigenvalues of the corresponding Jacobian matrix. Furthermore, from the equations $P(x_0, y_0) = 0$ and $Q(x_0, y_0) = 0$ for some given T, P_{CO} and E_3 we can find

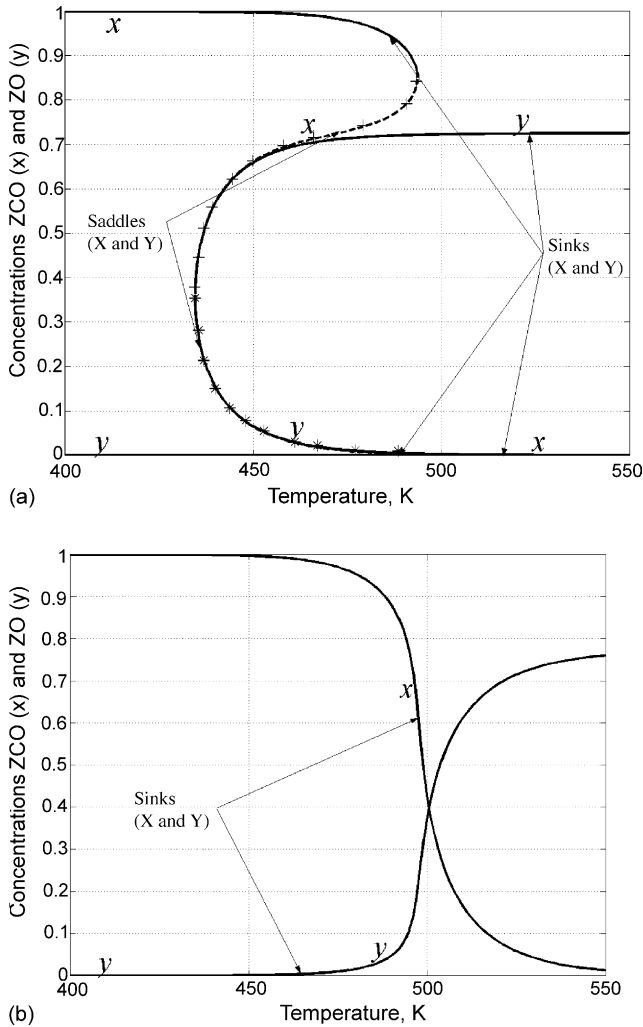


Fig. 3. Dependence of the steady states of the model (4) on the temperature at $E_3 = 28 \text{ kcal mol}^{-1}$ (a) and $E_3 = 33 \text{ kcal mol}^{-1}$ (b) for $P_{\text{CO}} = 1.1 \times 10^{-7} \text{ Torr}$, $P_{\text{O}_2} = 8 \times 10^{-7} \text{ Torr}$. Here the saddles are marked with + (x-coordinate) and * (y-coordinate).

explicitly the dependencies of the steady states coordinate $x_0 = x_0(y_0)$ and the oxygen partial pressure $P_{\text{O}_2} = P_{\text{O}_2}(x_0(y_0), y_0)$ on y_0 -coordinate, from which we have found all steady states for every P_{O_2} value by continuation along y_0 from 0 to 1.

From the Bendixon criterion [20], one can conclude that in the model (4) no oscillations of the reaction rate exist. Therefore, for description of the oscillating behavior we take into account the metallic surface modification over the course of reaction due to oxygen penetration into subsurface layers.

5. Mathematical model – II

Now we assume that when the adsorbed oxygen concentration y exceeds some critical value, a surface modification occurs and the reaction probability of absorbed oxygen with respect of CO changes, so that the activation energy E_3 of the

reaction stage (3) sharply increases [9]. Thus, we introduce a dependence $E_3 = E_3(y)$ into the model (4):

$$E_3(y) = \begin{cases} E_{31}, & y \leq y_c - \delta, \\ \tilde{E}(y), & |y - y_c| < \delta, \\ E_{32}, & y \geq y_c + \delta. \end{cases} \quad (5)$$

Here y_c and δ are two additional parameters that determine the location and width of the interval of adsorbed oxygen concentration y where an increase of the activation energy E_3 takes place. Here $E_3(y)$ is a smooth function such that $\tilde{E}(y_c - \delta) = E_{31}$, $\tilde{E}(y_c + \delta) = E_{32}$, $\tilde{E}(y_c) = 0.5(E_{31} + E_{32})$. In the paper we use the function $E_3(y)$ shown in Fig. 4 with $E_{31} = 28 \text{ kcal mol}^{-1}$ and $E_{32} = 33 \text{ kcal mol}^{-1}$. The difference between the maximum and minimum E_3 values was determined using the experimental data.

The addition of the stepwise dependence (5) emphasizes the reconstructive properties and phase singularities of the metallic surface layer [9–11]. The “step width” δ means the size of a transition region in respect to the y concentration where the increase of the modified surface part takes place, and the “step location” y_c is related to the affinity of the metallic surface with surface oxide.

Taking into account the dependence (5) of the activation energy E_3 on y we have obtained that for some intermediate values of temperature there exist one stable (a sink) and two unstable steady states (a saddle and a source) in the model (4). Furthermore, a stable periodic solution of a pronounced relaxation type can be found in the region Ω . It can be explained by the fact that after a coordinate system substitution to $(x + y, x - y)$ in a neighborhood of the limit cycle, a small parameter appears in (4), so that $d/dt(x - y) \gg d/dt(x + y)$. In Fig. 5, the phase plot of the system (4) is shown for the step-like function $E_3(y)$ with step width $2\delta = 0.2$ and center point at $y_c = 0.5$ (curve 2 and solid lines). In this case the single steady state (unstable source) exists in the region Ω and the oscillations are stable, so the system tends to the periodic

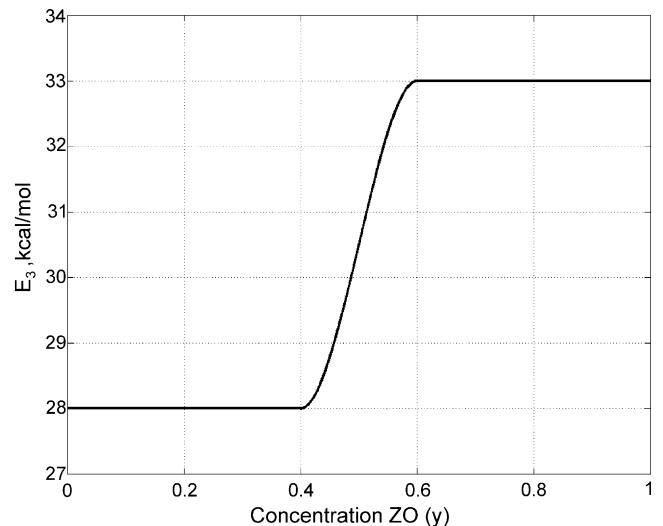


Fig. 4. Dependence of E_3 on y at $\delta = 0.1$, $y_c = 0.5$.

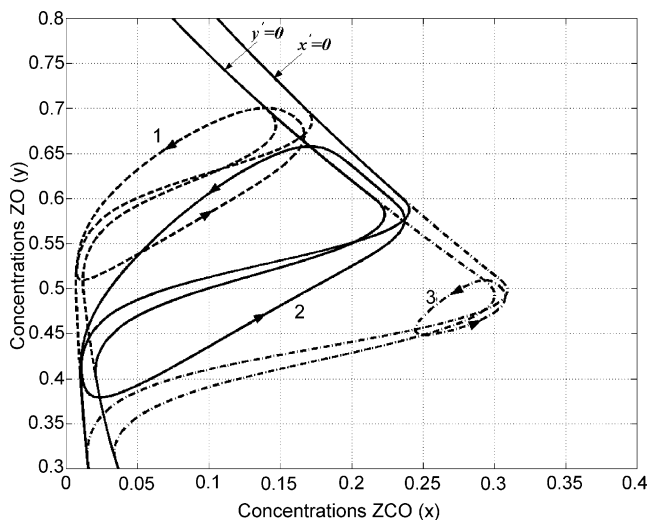


Fig. 5. Limit cycles (curves 1, 2 and 3) and null-clines of the model (4) and (5) for $T=500$ K, $P_{CO} = 1.1 \times 10^{-7}$ Torr, $P_{O_2} = 8 \times 10^{-7}$ Torr and $\delta = 0.1$ for $y_c = 0.6$ (dashed lines), 0.5 (solid lines), 0.41 (dash-dotted lines).

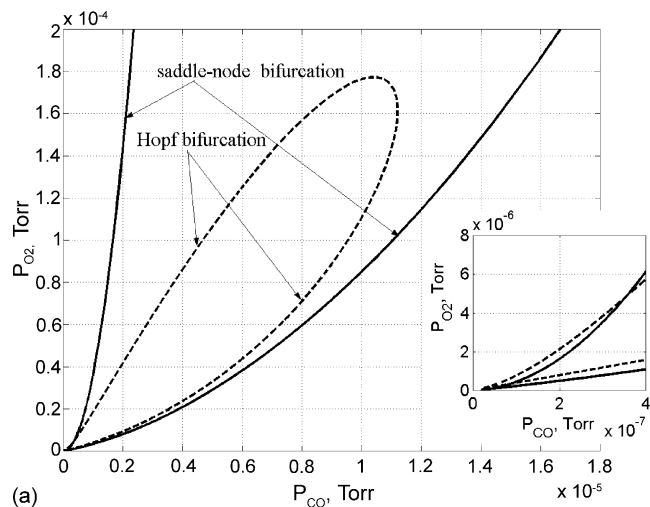
solution from any initial point. The periodic solution and its stability we have found based on the notion of the first return function or Poincaré map [20].

6. Local bifurcations of steady states and periodic solutions

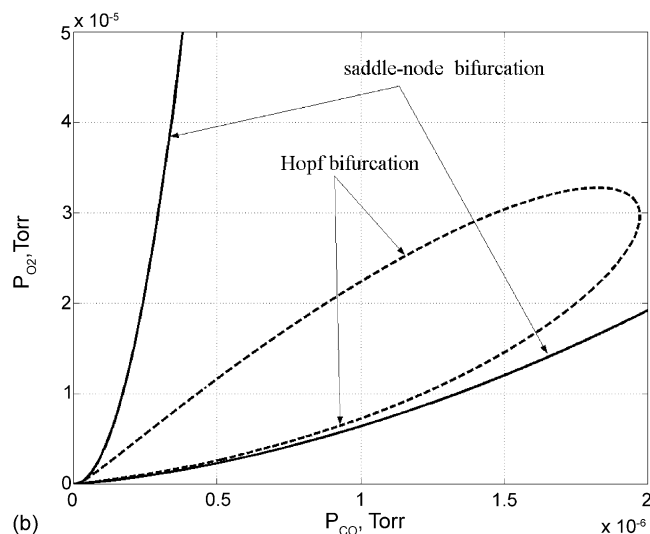
Construction of the bifurcation curves in the parametric plane (P_{CO} , P_{O_2}) under fixed temperature and function $E_3(y)$ allows us to find the areas of the partial CO and oxygen pressures, for which oscillations and/or steady states multiplicity in the model (4) and (5) occur.

The bifurcation curves [20] were constructed using y_0 as a parameter of continuation and the analytical dependencies of P_{CO} and P_{O_2} on y_0 . The Hopf bifurcation curve was found from the system $P(x_0, y_0) = 0$, $Q(x_0, y_0) = 0$ and $P_x(x_0, y_0) + Q_y(x_0, y_0) = 0$ with condition $P_x Q_y - P_y Q_x > 0$ at (x_0, y_0) . For the saddle-node bifurcation such dependence was found from equations $P(x_0, y_0) = 0$, $Q(x_0, y_0) = 0$ and $P_x Q_y - P_y Q_x = 0$ at (x_0, y_0) . Note that the bifurcation curves in the space (y_0, P_{CO}, P_{O_2}) do not intersect.

In Fig. 6, the curves of the saddle-node bifurcation and the Hopf bifurcation are shown for two different temperatures. For the values of P_{CO} and P_{O_2} from the area bounded by the “saddle-node bifurcation” curve, three steady states exist in the model (4) and (5). When the temperature decreases, for every fixed value of P_{CO} the maximum value of P_{O_2} and the length of the P_{O_2} interval for which three steady states exist, increase. For example, at $P_{CO} = 1.1 \times 10^{-7}$ Torr and $T = 470$ K maximum value of the partial pressures ratio P_{O_2}/P_{CO} is equal 38.5, and its minimum is 2.6. At $T = 500$ K and at the same CO partial pressure the interval of steady state multiplicity is $2.4 \leq P_{O_2}/P_{CO} \leq 5$ (see Fig. 6), while at $T = 510$ K it becomes more narrow and $2.3 \leq P_{O_2}/P_{CO} \leq 3$.



(a)



(b)

Fig. 6. Bifurcation curves for $\delta = 0.1$ and $y_c = 0.5$ at $T = 500$ K (a) and $T = 470$ K (b).

We have found that when the temperature decreases, the interval of P_{CO} values, for which the oscillations exist becomes more narrow and at $T = 400$ K the oscillations exist only for $P_{CO} < 1.2 \times 10^{-8}$ Torr. Let us denote by dP_{O_2} the length of the interval of P_{O_2} values for which the self-oscillations exist. For large values of P_{CO} , dP_{O_2} decreases with temperature. For example, the temperature decrease from 500 to 470 K leads to a decrease in dP_{O_2} for $P_{CO} \geq 1.3 \times 10^{-6}$ Torr, and to some increase of dP_{O_2} for $P_{CO} < 1.3 \times 10^{-6}$ Torr (Fig. 6).

7. Influence of parameters δ and y_c on self-oscillations

Now we discuss the influence of width δ and location y_c of the function $E_3(y)$ step change on the regions of existence of self-oscillations, their amplitude and period.

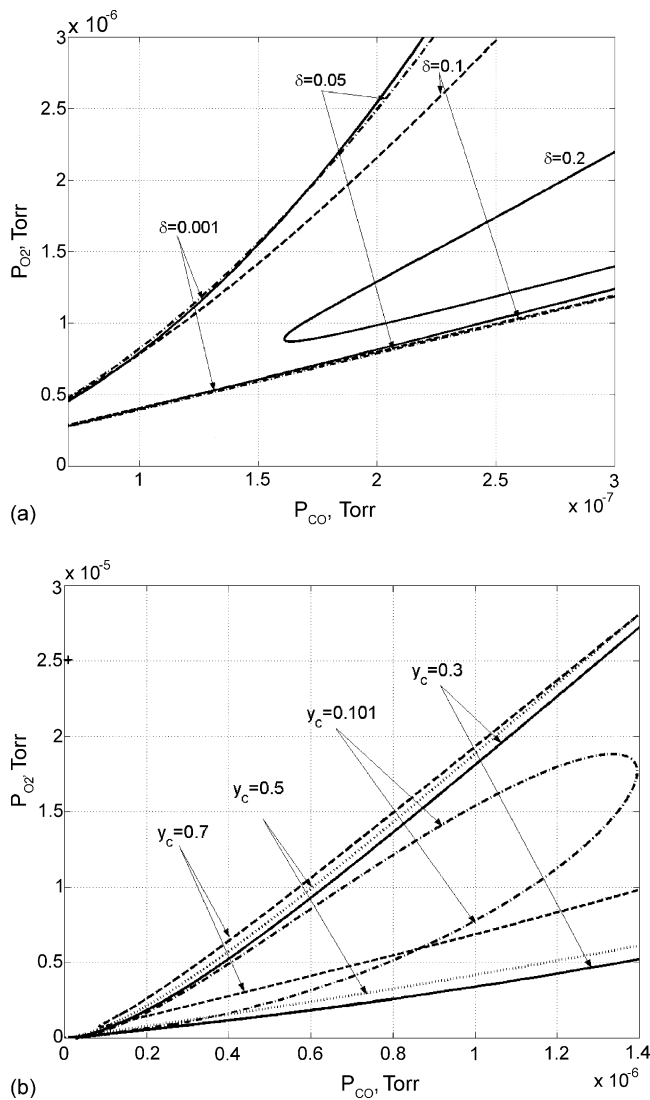


Fig. 7. Dependence of the Hopf bifurcation curves at $T=500$ K on the “step” width for $y_c=0.5$ (a) and on the “step” location for $\delta=0.1$ (b).

Studying the model (4) and (5) for different step width, we have obtained that for large δ increasing of E_3 occurs slowly, and oscillations exist for larger P_{CO} and P_{O_2} values. For example, for $T=500$ K and $\delta=0.2$, $y_c=0.5$, the oscillations exist for $P_{CO} > 1.6 \times 10^{-7}$ Torr (Fig. 7a). For fixed P_{CO} and temperature and decreasing δ , dP_{O_2} increases at first, and then decreases. The critical value $\delta = \delta^*$, for which dP_{O_2} starts to decrease, increases with P_{CO} decreasing. Furthermore, when δ decreases, the amplitude and period of oscillations grow, but averaged over the period values of adsorbed CO and oxygen concentrations are nearly constant. Some examples are given in Fig. 8. At $y_c=0.5$ and $\delta=0.13$ we obtain the self-oscillations with the period $T_{ps} = 113.566$ s, values of adsorbed CO and oxygen concentrations averaged over the period are $x_{av} = 0.185$ and $y_{av} = 0.591$. If $\delta=0.1$ the parameters of the periodic solution are as follows: $T_{ps} = 150.41$ s, $x_{av} = 0.1914$ and $y_{av} = 0.602$, while for $\delta=0.05$ they are $T_{ps} = 203.46$, $x_{av} = 0.2083$, and $y_{av} = 0.5911$. At $\delta=0.01$ and

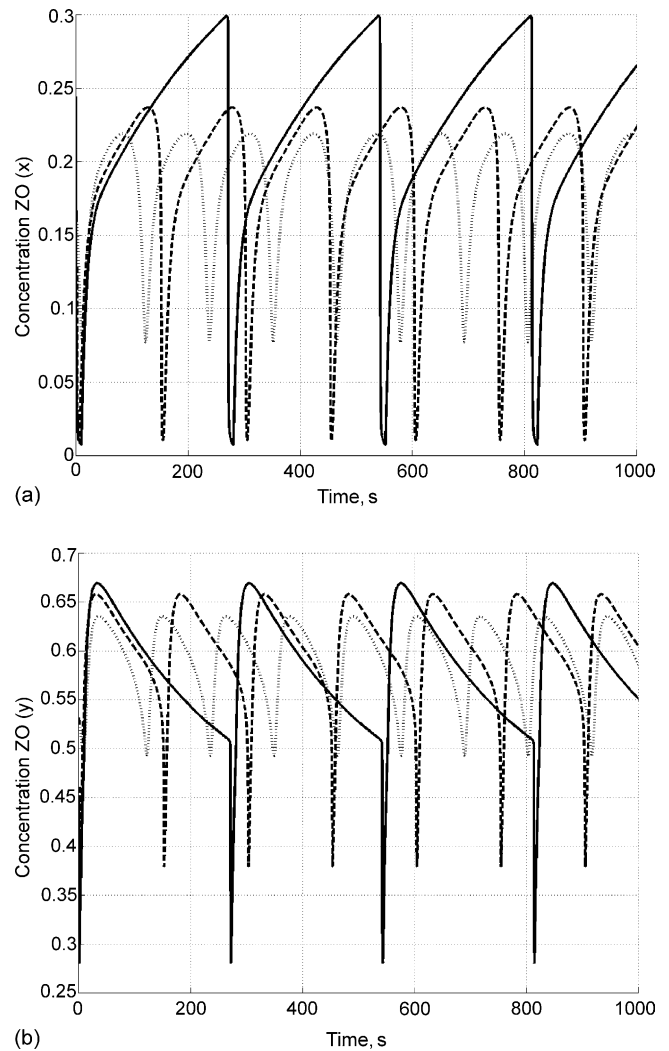


Fig. 8. Relaxation oscillations at $T=500$ K, $P_{CO}=1.1 \times 10^{-7}$ Torr, $P_{O_2}=8 \times 10^{-7}$ Torr and $y_c=0.5$: time dependence of x -coordinate (a) and y -coordinate (b) for $\delta=0.13$ (dotted lines), $\delta=0.1$ (dashed lines), $\delta=0.01$ (solid lines).

the same other parameters the period of self-oscillations is $T_{ps} = 271.02$ s and $x_{av} = 0.2238$, $y_{av} = 0.5769$.

Numerical study of the model (4) and (5) for different y_c has shown that for small y_c for fixed P_{CO} and T two intervals of P_{O_2} values exist, for which the oscillations appear in the region Ω . At one end of each interval the periodic solutions appear (or disappear) via the Hopf bifurcation, at the other end the disappearance (or appearance) of periodic orbits is associated with a global saddle loop bifurcation. For example, two families of the self-oscillations exist over a range of partial pressures P_{O_2} for $T=500$ K, $P_{CO}=1.1 \times 10^{-7}$ Torr, $y_c=0.1$ and $\delta=0.1$. The Hopf bifurcations occur at $P_{O_2} = 2.87457 \times 10^{-7}$ and 6.35257×10^{-7} Torr. The saddle-loop bifurcations occur at $P_{O_2} = 2.8849947 \times 10^{-7}$ and 3.7961515×10^{-7} Torr. Under increasing y_c these two intervals merge, the maximum and minimum of P_{O_2} and P_{CO} values, for which oscillations exist, are going up and then going down (see Fig. 7b). If y_c is

increasing, the region of self-oscillations moves up and to the right on the (P_{CO} , P_{O_2}) plane. And for $P_{\text{CO}} < 1.3 \times 10^{-7}$ Torr the maximum value of y_c , for which oscillations are observed in the model (4) and (5), decreases with decrease of P_{CO} . When P_{CO} increases above 1.3×10^{-6} Torr, the minimum value of y_c for which oscillations are observed increases.

From Fig. 5 it is obvious, that while y_c decreases, the amplitude of the oscillations increases, and then it decreases. For instance, the period of self-oscillations is $T_{\text{ps}} = 104.81$ s at $y_c = 0.4$, and $T_{\text{ps}} = 77.2$ s at $y_c = 0.6$, while at $y_c = 0.5$ the period $T_{\text{ps}} = 150.41$ s.

8. Conclusions

In this work the key role of the adsorbed oxygen, its influence on the catalyst surface properties and hysteresis phenomena appearance was determined.

Taking into account the modification of surface properties under reaction influence, we have suggested that the activation energy of interaction between the adsorbed oxygen and carbon monoxide sharply increases when the surface coverage by oxygen reaches some critical value. We present analysis of the nonlinear dynamics in a new two-variable kinetic model of the CO oxidation on the Ir surface.

This approach allows us to find the relaxation oscillations of the reaction rate in the mathematical model based on the conventional Langmuir–Hinshelwood mechanism.

The conducted analysis of two-variable kinetic model of CO oxidation over Ir catalyst in framework of this method gives us an approach for the description of the complex dynamics in models of greater dimension in the future.

References

- [1] M.M. Slinko, N.I. Jeager, Oscillating Heterogeneous Catalytic Systems, Stud. Surf. Sci. Catal, vol. 86, Elsevier, Amsterdam, 1994.
- [2] K. Krischer, M. Eiswirth, G. Ertl, Oscillatory CO oxidation on Pt (1 1 0): modeling of temporal self-organization, J. Chem. Phys. 96 (12) (1992) 9161–9172.
- [3] E.S. Kurkina, N.V. Peskov, M.M. Slinko, M.G. Slinko, About the nature of chaotic oscillations of the CO oxidation rate on Pd-zeolite catalyst, Dokl. Acad. Nauk 351 (4) (1996) 497–501 (in Russian).
- [4] E.S. Kurkina, E.D. Tolstunova, The general mathematical model of CO oxidation reaction over Pd-zeolite catalyst, Appl. Surf. Sci. 182 (2001) 72–90.
- [5] E.I. Latkin, V.I. Elokhin, V.V. Gorodetskii, Monte Carlo model of oscillatory CO oxidation having regard to the change of catalytic properties due to the adsorbate-induced Pt(1 0 0) structural transformation, J. Mol. Catal. A: Chem. 166 (1) (2001) 23–30.
- [6] G. Ertl, Heterogeneous catalysis on the atomic scale, Chem. Rec. 1 (1) (2001) 33–45.
- [7] A. Ramstad, F. Strisland, S. Raaen, A. Borg, C. Berg, CO and O₂ adsorption on the Re/Pt(1 1 1) surface studied by photoemission and thermal desorption, Surf. Sci. 440 (1–2) (1999) 290–300.
- [8] S. Ladas, S. Kennou, N. Hartmann, R. Imbihl, Characterisation of the oxygen adsorption states on clean and oxidized Ir(1 1 0) surfaces, Surf. Sci. 382 (1–3) (1997) 49–56.
- [9] A.I. Boronin, A.I. Nizovskii, Reaction of carbon monoxide oxidation over iridium, Mechanisms of adsorption and catalysis on clean metallic surfaces, Novosibirsk Institute of Catalysis, 1989, pp. 39–61 (in Russian).
- [10] V.I. Elokhin, A.I. Boronin, Modeling of CO+O₂ reaction on Ir, Mechanisms of adsorption and catalysis on clean metallic surfaces, Novosibirsk Institute of Catalysis, 1989, pp. 62–76 (in Russian).
- [11] A.I. Boronin, V.I. Elokhin, Dynamics of surface processes over iridium in carbon monoxide oxidation reaction, in: Proceedings of the First Soviet-Chinese Seminar on Catalysis, Novosibirsk, Institute of Catalysis, 1991, pp. 5–20.
- [12] G.A. Chumakov, M.G. Slinko, Kinetic turbulence (chaos) of reaction rate for hydrogen oxidation over metallic catalysts, Dokl. Acad. Nauk USSR 266 (5) (1982) 1194–1198 (in Russian).
- [13] G.A. Chumakov, N.A. Chumakova, Relaxation oscillations in a kinetic model of catalytic hydrogen oxidation involving a chase on canards, Chem. Eng. J. 91 (2–3) (2003) 151–158.
- [14] D. Briggs, M.P. Seach, Practical Surface Analysis by Auger and X-ray Photoelectron Spectroscopy, Wiley, New York, 1983.
- [15] G. Ertl, Surf. Sci. 299–300 (1994) 742–754.
- [16] T.A. Gruyters, D.A. King, Modeling temporal kinetic oscillations for CO oxidation on Pt(1 0 0). The (1 × 1)-CO island growth rate power law model, Chem. Phys. 232 (1–2) (1995) 1–6.
- [17] K.M. Khan, K. Yaldram, Surf. Sci. 445 (2000) 186–194.
- [18] I.Z. Jones, R.A. Bennett, M. Bowker, Surf. Sci. 445 (1999) 235–248.
- [19] F.P. Leizenberger, G. Koller, M. Sock, et al., Surf. Sci. 445 (2000) 380–393.
- [20] A.A. Andronov, E.A. Leontovich, I.I. Gordon, A.G. Maier, Theory of Dynamical Systems on a Plane, Nauka, Moscow, 1966 (in Russian).